Biochemical and Biophysical Research Communications 452 (2014) 701–707

Contents lists available at ScienceDirect

Biochemical and Biophysical Research Communications

journal homepage: www.elsevier.com/locate/ybbrc

# Suppression of Rad leads to arrhythmogenesis via PKA-mediated phosphorylation of ryanodine receptor activity in the heart

Hiroyuki Yamakawa [a], Mitsushige Murata [b,*], Tomoyuki Suzuki [c], Hirotaka Yada [d], Hideyuki Ishida [e], Yoshiyasu Aizawa [a], Takeshi Adachi [d], Kaichiro Kamiya [c], Keiichi Fukuda [a]

[a] Department of Cardiology, School of Medicine, Keio University, Tokyo, Japan
[b] Department of Laboratory Medicine, School of Medicine, Keio University, Tokyo, Japan
[c] Department of Cardiovascular Research, Research Institute of Environmental Medicine, Nagoya University, Nagoya, Japan
[d] Department of Cardiology, First Internal Medicine, National Defense Medical College, Saitama, Japan
[e] Department of Physiology, Tokai University School of Medicine, Kanagawa, Japan

ARTICLE INFO

*Article history:*
Received 18 August 2014
Available online 1 September 2014

*Keywords:*
Rad (Ras associated with diabetes)
Excitation–contraction (EC) coupling (ECC)
Ryanodine receptor
$Ca^{2+}$ imaging
PKA signaling

ABSTRACT

Ras-related small G-protein Rad plays a critical role in generating arrhythmias via regulation of the L-type $Ca^{2+}$ channel (LTCC). The aim was to demonstrate the role of Rad in intracellular calcium homeostasis by cardiac-Specific dominant-negative suppression of Rad. Transgenic (TG) mice overexpressing dominant-negative mutant Rad (S105N Rad TG) were generated. To measure intracellular $Ca^{2+}$ concentration ($[Ca^{2+}]_i$), we recorded $[Ca^{2+}]_i$ transients and $Ca^{2+}$ sparks from isolated cardiomyocytes using confocal microscopy. The mean $[Ca^{2+}]_i$ transient amplitude was significantly increased in S105N Rad TG cardiomyocytes, compared with control littermate mouse cells. The frequency of $Ca^{2+}$ sparks was also significantly higher in TG cells than in control cells, although there were no significant differences in amplitude. The sarcoplasmic reticulum $Ca^{2+}$ content was not altered in the S105N Rad TG cells, as assessed by measuring caffeine-induced $[Ca^{2+}]_i$ transient. In contrast, phosphorylation of $Ser^{2809}$ on the cardiac ryanodine receptor (RyR2) was significantly enhanced in TG mouse hearts compared with controls. Additionally, the Rad-mediated RyR2 phosphorylation was regulated via a direct interaction of Rad with protein kinase A (PKA).



## 1. Introduction

Rad (Ras associated with diabetes) is a member of the Ras-related Rad, Gem, and Kir (RGK) family of small GTP binding proteins, which was identified by subtractive cloning as overexpressed in skeletal muscle of patients with type 2 diabetes mellitus [1,2]. The RGK family encodes GTP-binding proteins with several structural features that are distinct from other GTPases [3,4]. Compared to Ras, the N-terminus of Rad is extended by 88 amino acids and the C-terminus is extended by 31 amino acids, and Rad lacks a CAAX-like prenylation site present in other Ras-like molecules [5,6]. These characteristic structures allow Rad to interact with a variety of cellular effectors to participate in many biological functions. Rad can inhibit insulin-stimulated glucose uptake in myocyte and adipocyte cell lines [6] and regulate neurite extension via Rho/RhoA kinase (ROK) signaling [7], and Rad expression is upregulated in vascular smooth muscle cells (VSMCs) during vascular lesion formation [8]. Regarding the role of Rad in the heart, we previously reported that Rad could function as a potent inhibitor of voltage-dependent calcium channels by directly binding to their β-subunit and that dominant-negative suppression of Rad induced ventricular arrhythmias [9]. Other groups have also reported the physiological importance of Rad in cardiac functions [9–11]. Chang et al. reported that Rad is downregulated in the human failing heart and knocking out Rad in mouse heart exaggerated cardiac hypertrophic remodeling under pressure overload conditions, via enhanced $Ca^{2+}$/calmodulin-dependent kinase II (CaMKII) signaling [10]. Rad also serves as an important endogenous regulator of cardiac excitation–contraction (EC) coupling and β-adrenergic signaling [11]. Together, these results including our study indicate that Rad may interact with a signaling pathway that regulates $Ca^{2+}$ homeostasis in cardiomyocytes, which may in turn influence arrhythmias as well as the remodeling of hypertrophy in hearts. However, the mechanism for Rad-mediated regulation of intracellular $Ca^{2+}$ homeostasis in cardiomyocytes has not been fully elucidated.

* Corresponding author. Address: Department of Laboratory Medicine, Keio University, 35 Shinanomachi, Shinjuku-ku, Tokyo 160-8582, Japan. Fax: +81 3 5363 3875.
*E-mail address:* muratam@a7.keio.jp (M. Murata).

http://dx.doi.org/10.1016/j.bbrc.2014.08.126
0006-291X/

The main goal of this study was therefore to examine the effect of Rad on cardiac intracellular calcium homeostasis and to clarify its mechanisms using an *in vivo* mouse model of cardiac-specific dominant-negative suppression of Rad.

## 2. Methods

All experimental procedures and protocols were approved by the Animal Care and Use Committee of Keio University (20-041-4) and conformed to the NIH Guide for the Care and Use of Laboratory Animals (NIH Publication No. 85-23 revised 1996).

### 2.1. Adenoviral transduction and cell culture

Ventricular cardiomyocytes were isolated from the left ventricles of adult mice using enzymatic digestions as previously described, with slight modifications [9]. Isolated cardiomyocytes were re-suspended in Dulbecco's modified Eagle's medium (DMEM) containing 10% fetal bovine serum (FBS) and 1% penicillin–streptomycin (all from Invitrogen, Carlsbad, CA) and then plated at a density of $6 \times 10^5$/dish. Adenovirus harboring Ad-GFP and Ad-S105N Rad was added to the culture medium of cardiomyocytes. Cultured cardiomyocytes of Ad-GFP and Ad-S105N Rad were utilized as electrophysiological and biochemical measurements 24 h after infection.

### 2.2. Electrophysiological experiments

The L-type calcium current ($I_{Ca,L}$) and action potential were recorded using the whole-cell patch clamp technique with an Axopatch 200B amplifier (Axon Instruments, Foster City, CA). All recordings from myocytes were performed at 37 °C. Cells were superfused in solution containing (in mmol/L) 140 NaCl, 5 KCl, 1 $MgCl_2$, 10 HEPES, 2 $CaCl_2$, and 10 glucose (pH 7.4, adjusted with NaOH). For $I_{Ca,L}$ recordings, the external solution was replaced with a $Na^+$, $K^+$-free solution after establishing the whole-cell clamp mode. The micropipette electrode solution for measuring $I_{Ca,L}$ was composed of (in mmol/L) 60 CsOH, 80 CsCl, 40 asparate, 5 HEPES, 10 EGTA, 5 MgATP, 5 phosphocreatinine, and 0.65 $CaCl_2$. L-type calcium currents were elicited by 300-ms depolarizing steps from −40 to 65 mV, in 5-mV increments.

Action potentials (APs) were recorded in an external solution containing (in mmol/L) 140 NaCl, 5 KCl, 1 $MgCl_2$, 10 HEPES, 1.8 $CaCl_2$, and 10 glucose (pH 7.4, adjusted with NaOH). The micropipette electrode solution for recording action potentials was composed of (in mmol/L) 130 K-glutamate, 9 KCl, 10 HEPES, 2 EGTA, and 5 MgATP (pH 7.2, adjusted with KOH). Action potentials were initiated by short depolarizing current pulses (2–3 ms, 500–800 pA) at 2 Hz. $Ba^{2+}$ currents were recorded at 25 °C in an external solution containing (in mmol/L) NaCl 140, CsCl 5, $BaCl_2$ 4, $MgCl_2$ 1.0, glucose 10, and HEPES 10 (pH 7.4, adjusted with NaOH).

### 2.3. Calcium imaging experiments

Initially, myocytes were loaded at 37 °C with Fluo-4 AM (10 μM; Molecular Probes) for 30 min to measure $[Ca^{2+}]_i$ transient, $Ca^{2+}$ spark, and $Ca^{2+}$ wave. The cells were then assessed for Fluo-4 fluorescent signal intensity at room temperature using a Zeiss LSM-510 confocal microscope (5-Live mode) with a × 40 lens (NA 1.3) and laser excitation/emission (488/543 nm) [12]. Myocytes were incubated in 1.0 mM $Ca^{2+}$ Tyrode solution and stimulated via platinum electrodes connected to a stimulator at a frequency of 1 Hz. Contraction amplitudes and rates of contraction and relaxation were recorded online with a video edge-detection system and data acquisition software as described previously [12]. The sarcoplasmic reticulum (SR) $Ca^{2+}$ content was evaluated after rapid injection of caffeine (10 mM) [13] and expressed as a relative value of the baseline value, $F/F_0$.

### 2.4. Western blotting

Total protein was extracted from frozen hearts. Equal amounts of total extracted protein (20–50 μg) were subjected to SDS–PAGE. A rabbit anti-Rad polyclonal antibody (a kind gift from Ronald Kahn in the Joslin Diabetes Center, Harvard Medical School) was used for Rad detection. The other primary antibodies were purchased as follows: anti-cardiac $Ca^{2+}$ ATPase (SERCA2a), anti-phospholamban (PLB), and anti-phospho-PLB $Ser^{16}$ (p-PLB $Ser^{16}$) (Affinity BioReagents); anti-$Na^+/Ca^{2+}$ exchanger (NCX) (Abcam); anti-RyR2, anti-phospho-RyR $Ser^{2809}$ (p-RyR $Ser^{2809}$), anti-PKA-C (PKA catalytic subunit), and anti-phospho-PKA C $Thr^{197}$ (p-PKA C $Thr^{197}$) (Cell Signaling Technology); anti-β1 AR and anti-β2 AR (Sigma–Aldrich).

### 2.5. PKA kinase assay

The samples of heart tissues (about each 10 g) were homogenized in 1 ml of 0.1 N HCl. The lysates were centrifuged at 1200*g* for 10 min at 4°. The supernatants were assayed immediately. The concentrations of cAMP were measured using a radioimmunoassay kit (Yamasa).

### 2.6. Statistical analysis

All data are shown as mean ± SEM. Statistical differences were determined using repeated-measures ANOVA, and $P < 0.05$ was considered significant.

## 3. Results

### 3.1. Dominant-negative suppression of Rad in cardiomyocytes leads to the induction of triggered activities

To first confirm the dominant-negative Rad effect on $I_{Ca,L}$ in genetically modified mouse cells, we measured $I_{Ca,L}$ from wild-type littermates (control) and S105N Rad TG mouse cardiomyocytes using whole-cell patch clamping in voltage clamp mode. Fig. 1A shows representative $I_{Ca,L}$ traces recorded from control and S105N Rad TG cardiomyocytes. The peak $I_{Ca,L}$ was dramatically larger in the S105N Rad TG cells than in controls (15.9 ± 1.0 pA/pF at 5 mV ($n = 4$) in S105N Rad vs 9.4 ± 0.9 pA/pF at 5 mV ($n = 8$) in control, Fig. 1A). In contrast, there were no significant differences in steady-state inactivation curves ($n = 7$) and activation curves ($n = 8$) between these groups (Fig. 1B).

Next, we recorded the action potentials (APs) in current-clamp mode. Fig. 1C shows representative AP traces from control and S105N Rad TG cells. Both AP durations were significantly prolonged at 50% repolarization ($APD_{50}$) and at 90% ($APD_{90}$) in S105N Rad TG cells, compared with control cells ($APD_{90}$: 53.2 ± 7.3 ms ($n = 4$) in S105N Rad vs 30.8 ± 4.6 ms ($n = 7$) in control, Fig. 1D). Consistent with the prolongation of APDs in S105N Rad TG cells, the abnormal potentials like triggered activities including delayed after depolarizations (DADs) and early after depolarizations (EADs) were observed in S105N Rad TG cells (Fig. 1E), while no abnormal activities were observed in controls, implicating the intracellular $Ca^{2+}$ overload by downregulation of Rad activity.

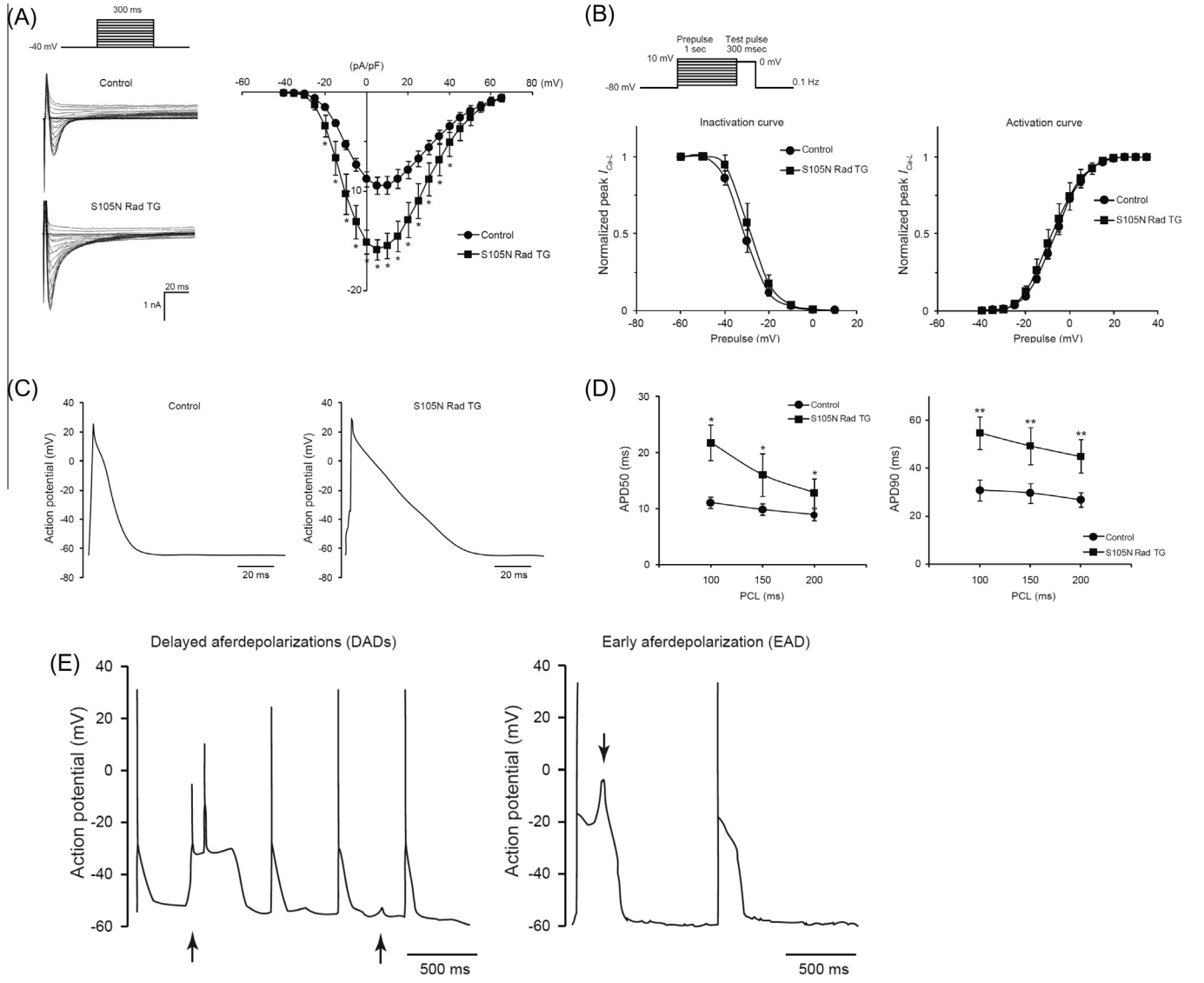


**Fig. 1.** The electrophysiological properties in S105N Rad TG mice. (A) Representative $I_{Ca,L}$ in control and dominant negative Rad (S105N Rad) TG mouse (left panel). The peak $I_{Ca,L}$ was dramatically larger in the S105N Rad TG cells than in controls (right panel $-15.9 \pm 1.0$ pA/pF at 5 mV ($n = 4$) in S105N Rad vs $-9.4 \pm 0.9$ pA/pF at 5 mV ($n = 8$) in control; $P < 0.01$). (B) The effect of Rad activity on activation and inactivation curves in $I_{Ca,L}$ (inactivation curves (left panel) and activation curves (left panel)). There were no significant differences in steady-state inactivation curves among these groups ($n = 7$) and in steady-state inactivation curves among these groups ($n = 8$). (C) Representative action potential traces recorded from control and S105N Rad TG mouse cardiomyocytes. (D) Action potential duration at 50% repolarization ($APD_{50}$) and at 90% ($APD_{90}$). $APD_{50}$ in S105N Rad TG was significantly prolonged compared with control cells ($APD_{50}$ at the pacing length of 100 ms: $21.7 \pm 3.2$ ms ($n = 7$) in S105N Rad cells vs $11.1 \pm 1.6$ ms ($n = 7$) in controls; $P = 0.02$). $APD_{90}$ in S105N Rad TG was significantly prolonged compared with control cells ($APD_{90}$ at the pacing length of 100 ms: $54.7 \pm 6.8$ ms ($n = 7$) in S105N Rad cells vs $30.8 \pm 4.6$ ms ($n = 7$) in controls; $P = 0.04$). (E) Triggered activities in S105N Rad. Delayed afterdepolarization (DAD) was observed in S105N Rad TG mouse (left panel). Early afterdepolarization (EAD) was also observed in S105N Rad (right panel). However, no abnormal activities were observed in control cells.

### 3.2. Rad regulates intracellular $Ca^{2+}$ homeostasis in cardiomyocytes

To evaluate $Ca^{2+}$ overload in S105N Rad TG mice, we investigated the effects of Rad on intracellular $Ca^{2+}$ concentration using $Ca^{2+}$ indicator, Fluo-4 AM. Fig. 2A and B show the representative line scan images, and their corresponding $[Ca^{2+}]_i$ transients by field stimulation at 1 Hz in cardiomyocytes obtained from control and S105N Rad TG mice. The amplitude of $[Ca^{2+}]_i$ transients ($F/F_0$) was larger in S105N Rad TG cell than in controls, showing a mean increase of 34%. In contrast, there were no significant differences in decreased time to 50% relaxation (RT50) or the tendency for a decrease of the time constant ($\tau$ of $[Ca^{2+}]_i$ decline in cardiomyocytes, which was indicated as the index of relaxation (Fig. 2C). A possible mechanism for the effect of Rad on the $[Ca^{2+}]_i$ transient amplitudes could involve the regulation of SR $Ca^{2+}$ content. To clarify this possibility, we measured caffeine-evoked $[Ca^{2+}]_i$ transients; however, there were no significant differences in the amplitude, $\tau$, or RT50 of $[Ca^{2+}]_i$ transients between S105N Rad TG and control cells (Fig. 2D).

The spatial and temporal uniformity of $Ca^{2+}$ transients are important aspects of cardiac EC coupling and its modulation by β-AR stimulation [14]. In heart failure models, dis-synchronous SR $Ca^{2+}$ releases, such as $Ca^{2+}$ sparks and waves, have also been linked to reduced inotropy and enhanced arrhythmogenesis [15]. To investigate the $Ca^{2+}$ leak in S105N Rad TG mice, we therefore recorded $Ca^{2+}$ sparks emitted from isolated S105N Rad TG and control cardiomyocytes (Fig. 2E). The frequency of $Ca^{2+}$ sparks, $F/F_0$ and full duration at half maximum (FDHM) of $Ca^{2+}$ sparks were increased in S105N Rad TG cardiomyocytes, compared with controls (Fig. 2F), while there were no significant

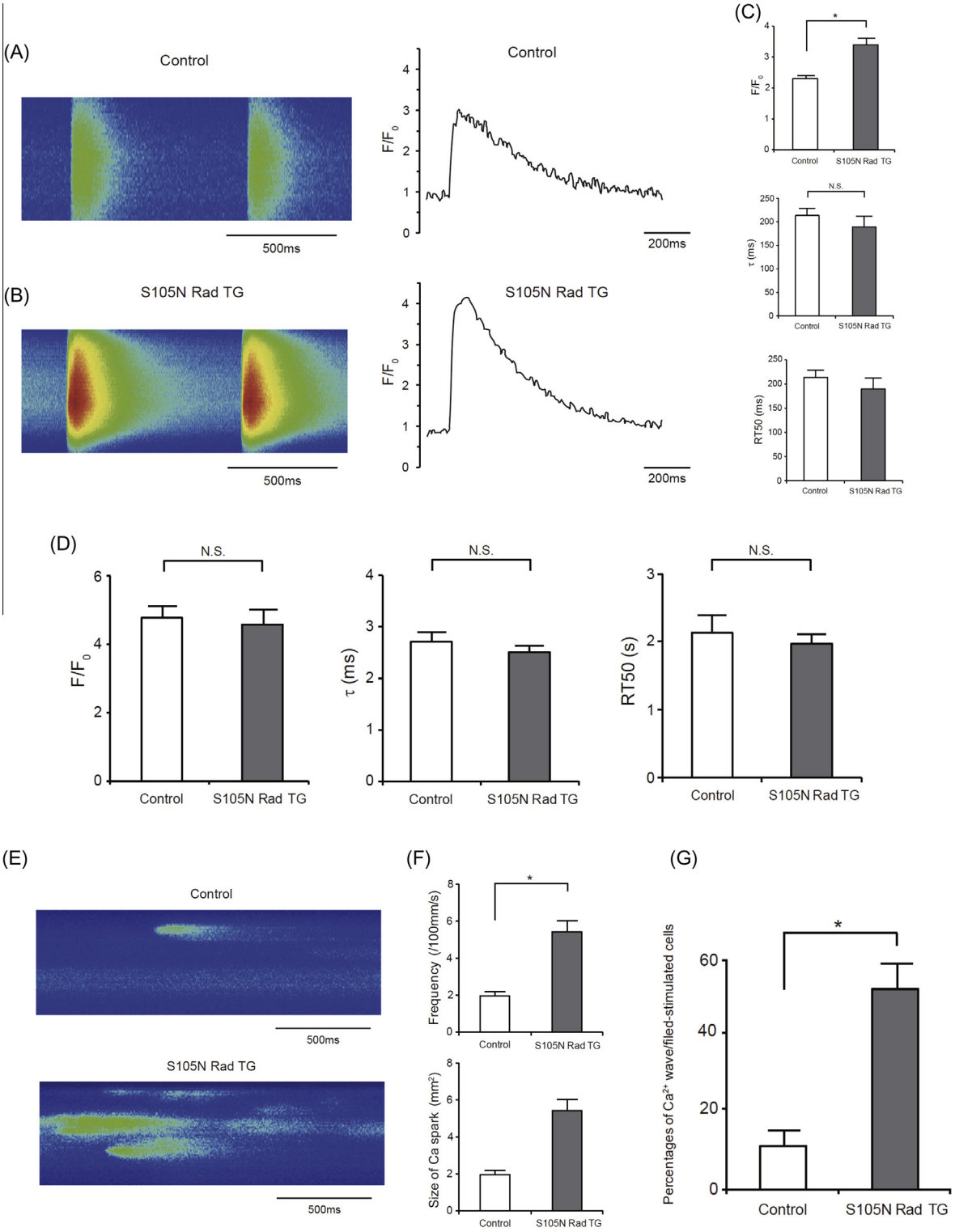


**Fig. 2.** Intracellular $Ca^{2+}$ imagings of S105N Rad TG mouse and control. The Representative line scan images and their $[Ca^{2+}]_i$ transients by field stimulation at 1 Hz recorded from control (A) and S105N Rad TG cardiomyocytes (B). (C) The parameters of $[Ca^{2+}]_i$ transients (control ($n = 25$) vs S105N Rad TG ($n = 25$), $^*P < 0.05$ vs control). (D) Amplitudes, RT50, and $\tau$ of $Ca^{2+}$ transients in response to rapid application of 10 mmol/l caffeine (control ($n = 46$) vs S105N Rad TG ($n = 47$)). (E) Representative traces of $Ca^{2+}$ sparks between control and S105N Rad TG cardiomyocytes. (F) Parameters of $Ca^{2+}$ sparks (control ($n = 30$) vs S105N Rad TG ($n = 32$), $^*P < 0.05$ vs control). The frequency of $Ca^{2+}$ sparks, $F/F_0$ and full duration at half maximum (FDHM) of $Ca^{2+}$ sparks were increased in S105N Rad TG cardiomyocytes, compared with controls (control ($n = 18$) vs S105N ($n = 24$), $^*P < 0.05$ vs control), while there were no significant differences in full width at half maximum (FWHM). (G) Percentages of spontaneous $Ca^{2+}$ waves in control and S105N Rad TG cardiomyocytes (control ($n = 330$) vs S105N ($n = 315$), $^*P < 0.05$ vs control).

differences in full width at half maximum (FWHM) (Fig. 2F). Notably, spontaneous $Ca^{2+}$ waves were more frequently observed in S105N Rad TG cells than in controls, and there was approximately 3-fold more cardiomyocytes induced with spontaneous $Ca^{2+}$ waves from S105N Rad mice compared to controls (Fig. 2G).

### 3.3. The phosphorylation of RyR-Ser$^{2809}$ was upregulated in S105N Rad TG mice

To investigate the mechanism behind the increased frequency of the SR $Ca^{2+}$ release channel, the phosphorylation of RyR2 at Serine 2809 (p-RyR2 Ser$^{2809}$) was examined, with the results showing a significant increase in p-RyR2 Ser$^{2809}$ in S105N Rad TG mice compared with control mice (Fig. 3A).

Furthermore, in order to exclude the non-specific increase in the phosphorylation of RyR2 in genetically S105N Rad TG mouse hearts, we measured the phosphorylation of p-RyR2 Ser$^{2809}$ in S105N Rad-transduced cardiomyocytes using adenoviral vectors. Consistent with *in vivo* mouse experiments, p-RyR2 Ser$^{2809}$ was significantly increased in S105N Rad-transduced cells (Ad S105N Rad cells), compared with cells transduced with control adenovirus (Ad-control cells). In contrast, there was no difference in the saturated level of p-RyR2 Ser$^{2809}$ stimulated with 1 μmol/L isoproterenol (ISO) between them (Fig. 3B). These results indicated that dominant negative suppression of Rad in the heart led to the upregulation of RyR2 activity.

### 3.4. Rad regulates the PKA signaling pathway

Since the site of Serine 2809 at RyR2 is a phosphorylation point of protein kinase A (PKA) [16,17], we investigated the phosphorylation of PKA. As shown in Fig. 3C, phosphorylated PKA-catalytic subunit at Thr$^{197}$ site (p-PKA-C Thr$^{197}$) was significantly greater in S105N Rad TG mice, compared with control. Furthermore, PKA kinase assay confirmed the upregulation of p-PKA-C Thr$^{197}$ in S105N Rad TG mice (Fig. 3D).

In order to elucidate the possibility of direct interaction between Rad and PKA, GST pull-down assay was performed. As shown in Fig. 4A, GST WT-Rad interacted with PKA-C, suggesting that the direct interaction of Rad on PKA might lead to the regulation of PKA as well as RyR2 phosphorylation.

There are several upstream molecules of PKA signaling pathway, including β-adrenergic receptors (β-ARs), adenylate cyclase (AC), and cAMP. We measured the concentration of cAMP, protein expression of β1-AR as well as β2-AR from whole hearts, and serum catecholamine. There were no significant differences in the concentration of cAMP and serum catecholamine, as well as expression of β-ARs (Fig. 4B–D).

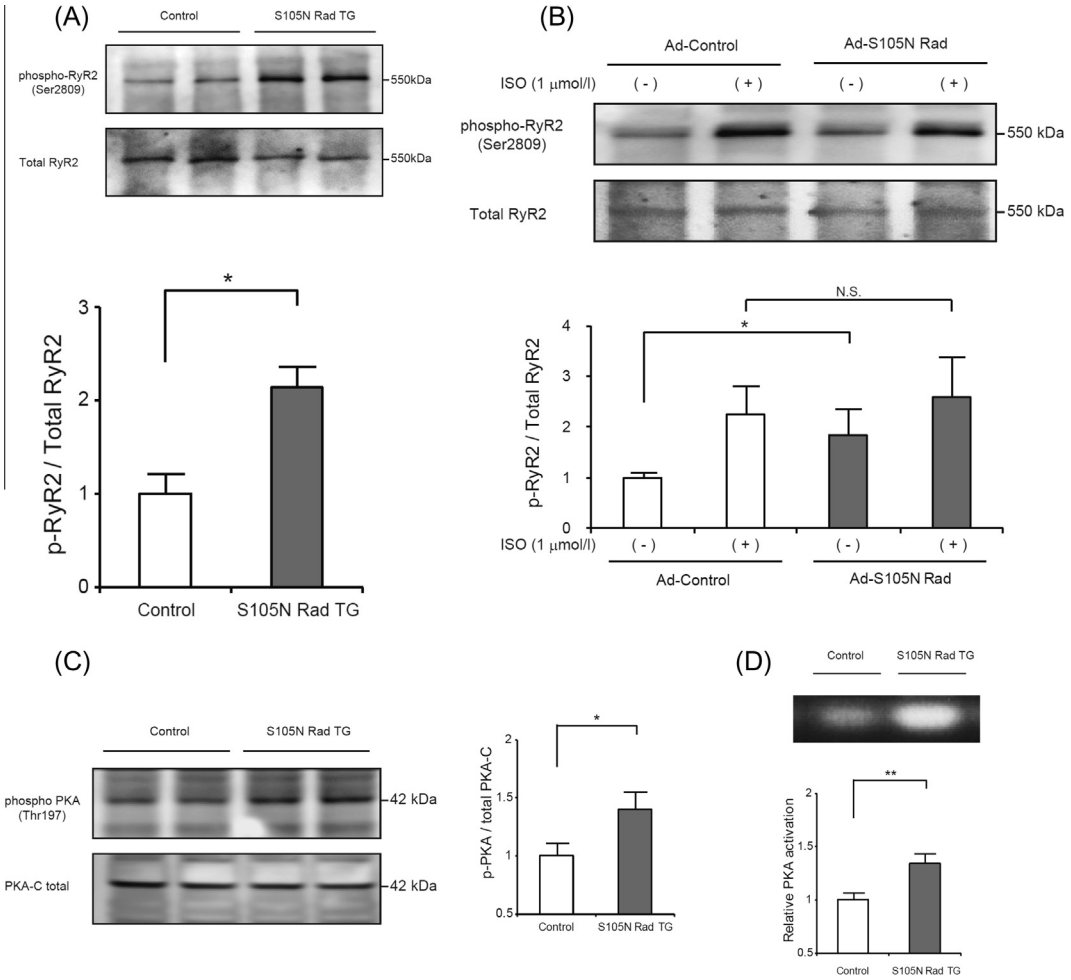


**Fig. 3.** Phosphorylation of RyR2 and PKA. (A) Western blots of phospho-ryanodine receptor 2 (RyR2) at Ser$^{2809}$ and total RyR2 protein in control and S105N Rad TG mouse hearts. Phosphorylation of RyR2 at Ser$^{2809}$ normalized with total RyR2 protein was significantly enhanced in S105N Rad TG hearts compared with controls ($n = 4$ for both; $^{*}P < 0.05$ vs control). (B) Western blots of p-RyR2 at Ser$^{2809}$ and total RyR2 protein in isolated adult cardiomyocytes transfected with Ad-GFP or Ad-S105N Rad. The cardiomyocytes overexpressing S105N-Rad showed higher levels of phosphorylation, compared with GFP overexpression alone. Treatment with 1 μM isoproterenol (ISO) abolished the observed change in phosphorylation of Ser$^{2809}$ RyR2 between Ad-GFP and Ad-S105N Rad overexpression (3 independent experiments, $^{*}P < 0.05$ vs control). (C) Western blots of total PKA (PKA-Total) and phosphorylated PKA catalytic subunit at Thr197 (p-PKA-C Thr$^{197}$) in S105N-Rad TG hearts and controls (4 independent experiments, $^{*}P < 0.05$ vs control). (D) PKA kinase assay of total PKA (PKA-Total) and p-PKA-C Thr$^{197}$ in S105N-Rad TG hearts and controls (3 independent experiments, $^{*}P < 0.05$ vs control).

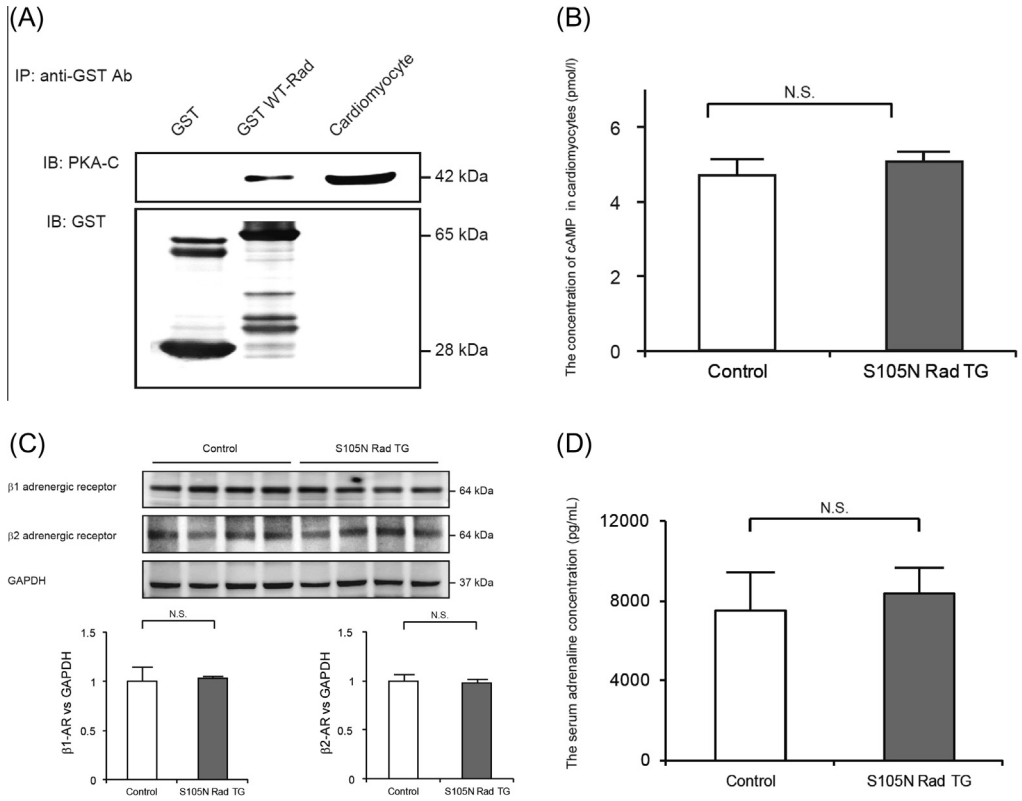


**Fig. 4.** PKA activity and cAMP/PKA signaling in S105N Rad heart. (A) GST-pull-down assay with immunoblotting of the antibody of PKA-C and GST, implicating the interaction between Rad and PKA-C. (B) Concentration of cAMP in S105N-Rad TG and control hearts (control ($n = 6$) vs S105N Rad TG ($n = 12$). (C) Western blots of β1-AR and β2-AR protein in S105N Rad TG and control hearts (control ($n = 8$) vs S105N Rad TG ($n = 8$). (D) The serum adrenaline concentration in S105N Rad TG mice and controls (control ($n = 5$) vs S105N Rad TG ($n = 5$)).

The other crucial signaling pathway that regulates RyR activity is a calmodulin-dependent kinase II (CaMKII) pathway. However, there were no significant changes in CaMKII phosphorylation between control and S105N Rad TG hearts (data not shown).

We finally analyzed the protein and messenger RNA (mRNA) expression levels of a range of these proteins from S105N Rad TG and control mice. Immunoblots of $Ca^{2+}$ handling proteins showed no significant differences in the protein expressions of SERCA2a, PLB, and NCX between control and S105N Rad TG hearts, while phosphorylated PLB at Serine 16, which is a PKA phosphorylation site, was increased in S105N Rad TG samples (data not shown).

## 4. Discussion

This is the first report to show that Rad could regulate SR $Ca^{2+}$ release channel activity via direct interaction with a PKA catalytic subunit. In this study, we found that ablation of Rad activity in a dominant-negative manner increased the amplitude of $[Ca^{2+}]_i$ transients as well as the frequency of $Ca^{2+}$ sparks, resulting in abnormal cellular excitability including triggered activities (EADs and DADs) and $Ca^{2+}$ waves. Consistent with this, the RyR2 activity was increased by dominant-negative suppression of Rad. The mechanism for this might be at least in part due to the upregulation of PKA signaling via direct interaction between Rad and a PKA catalytic subunit.

### *4.1. Rad regulates excitation–contraction coupling via upregulation of RyR2 activity*

Reduction of Rad activity in S105N Rad TG cardiomyocytes led to the significant increase in the amplitude of peak $I_{Ca,L}$ as well as $[Ca^{2+}]_i$ transients, compared with wild-type littermate mouse control cells. Furthermore, the frequency of $Ca^{2+}$ sparks was also significantly enhanced in S105N Rad TG cardiomyocytes. In contrast, there was no significant difference in caffeine-evoked $[Ca^{2+}]_i$ transients between control and S105N Rad TG cardiomyocytes, suggesting that Rad-mediated modulation of the $[Ca^{2+}]_i$ transient and $Ca^{2+}$ spark were not attributable to the changes in SR $Ca^{2+}$ content. Therefore, we investigated the activity of SR $Ca^{2+}$ release channel RyR2, and found that p-RyR2 $Ser^{2809}$ was significantly upregulated by the suppression of Rad activity in mouse hearts as well as at the single-cell level. Dysfunctional $Ca^{2+}$ handling proteins such as L-type $Ca^{2+}$ channel and RyR2 in the S105N Rad TG mice could induce intracellular $Ca^{2+}$ overload, and also induction of ventricular arrhythmias due to the changes in triggered activities shown herein and in our previous report [9].

In contrast to Wang et al., whose data demonstrated that Rad downregulation did not change the properties of $Ca^{2+}$ sparks and $Ca^{2+}$ wave frequency, our data clearly showed an increased frequency of $Ca^{2+}$ sparks and $Ca^{2+}$ wave in S105N Rad TG cardiomyocytes, compared with control cells [11]. The possible explanation for this discrepancy is that the cardiomyocytes used in the present study were freshly isolated and thus retained many necessary signal transduction molecules that may be downregulated during cell culture, as used in the previous report. According to their data, $Ca^{2+}$ spark frequency tended to be greater in Rad-downregulated cells compared with controls, although there were no significant differences. Wang et al. also demonstrated that β-adrenergic stimulation by ISO did not restore Rad-mediated inhibition of $I_{Ca,L}$ [11], whereas $I_{Ca,L}$ could be enhanced in Rad-downregulated cells, supporting our data that Rad may inhibit PKA phosphorylation via direct interaction with a PKA catalytic subunit. Taken together,

several distinct mechanisms for RGK-mediated L-type $Ca^{2+}$ channel regulation have been proposed in cardiomyocytes as followed: (1) channel trafficking, (2) reduction of channel-open probability, and (3) phosphorylation by PKA. However, the predominant mechanism underlying the regulation of L-type $Ca^{2+}$ channels may depend on experimental conditions including cell type, use of cultured cells, and disease states, and further studies are clearly warranted.

### *4.2. Rad directly interacts with PKA and regulates PKA signaling*

RyR2 is regulated by many signaling molecules including protein kinases (eg., calmodulin dependent kinase II, PKA, channel stabilizing protein calstabin2, protein phosphatases, and sorcin). Among these molecules, PKA can phosphorylate RyR2 at Serine 2809 [16,17], and an association of Rad with β-adrenergic signaling was implicated previously [11], and interactions between Rad and the β-adrenergic pathway were suggested. Although there were no significant differences in the expression of adrenergic receptor, cAMP levels, or the concentration of catecholamines between S105N Rad and control hearts, the phosphorylation of PKA was significantly increased in S105N Rad hearts and cardiomyocytes. Finally, PKA acts downstream of β-adrenergic signaling and upstream of RyR2 $Ser^{2809}$. Notably, the GST-pulldown assay in this study revealed for the first time a direct interaction of Rad with PKA catalytic subunits. Thus, the hyperphosphorylation of L-type $Ca^{2+}$ channels by PKA might contribute to the Rad-mediated increase in $I_{Ca,L}$ in addition to the channel trafficking regulation, as consistent with Rem-induced regulation of $I_{Ca,L}$ [18]. However, such a contribution would not have much of an impact because no changes were observed in the steady-state activation and inactivation of L-type $Ca^{2+}$ channels between S105N Rad TG and control cells. Thus, this study provided no significant evidence for upregulation of the activities of other PKA substrates including phospholamban and SERCA2a. We speculate that another molecule might be required in the interaction between Rad and PKA. One candidate for this is a PKA scaffolding protein, which could ensure that PKA accesses its phosphorylation substrate correctly. The association of Rad with PKA might therefore be regulated according to the interaction sites and other interacting molecules, and further studies are needed to investigate this hypothesis.

## Sources of funding

This work was supported by a Japanese Grant-in-Aid for Scientific Research (C) (to M. Murata).

## Disclosure

None.

## Acknowledgments

We thank Dr. Kouji Shimoda for production of transgenic mice, and Mika Mizusawa, Takako Koshiba and Emi Iida for technical assistance.

## References

[1] C. Reynet, C.R. Kahn, Rad: a member of the Ras family overexpressed in muscle of type II diabetic humans, Science 262 (1993) 1441–1444.
[2] D.E. Moller, C. Bjorbaek, A. Vidal-Puig, Candidate genes for insulin resistance, Diabetes Care 19 (1996) 396–400.
[3] J. Maguire, T. Santoro, P. Jensen, U. Siebenlisr, J. Yewdell, K. Kelly, Gem: an induced, immediate early protein belonging to the Ras family, Science 265 (1994) 241–244.
[4] L. Cohen, R. Mohr, Y.-Y. Chen, M. Huang, R. Kato, D. Dorin, et al., Transcriptional activation of a ras-like gene (kir) by oncogenic tyrosine kinases, Proc. Natl. Acad. Sci. U.S.A. 91 (1994) 12448–12452.
[5] J.A. Glomset, C.C. Farnsworth, Role of protein modification reactions in programming interactions between ras-related GTPases and cell membranes, Annu. Rev. Cell Biol. 10 (1994) 181–205.
[6] J.S. Moyers, P.J. Bilan, J. Zhu, C.R. Kahn, Rad and Rad-related GTPases interact with calmodulin and calmodulin-dependent protein kinase II, J. Biol. Chem. 272 (1997) 11832–11839.
[7] Y. Ward, S.-F. Yap, V. Ravichandran, F. Matsumura, M. Ito, B. Spinelli, et al., The GTP binding proteins Gem and Rad are negative regulators of the Rho–Rho kinase pathway, J. Cell Biol. 157 (2002) 291–302.
[8] M. Fu, J. Zhang, Y.-H. Tseng, T. Cui, X. Zhu, Y. Xiao, et al., Rad GTPase attenuates vascular lesion formation by inhibition of vascular smooth muscle cell migration, Circulation 111 (2005) 1071–1077.
[9] H. Yada, M. Murata, K. Shimoda, S. Yuasa, H. Kawaguchi, M. Ieda, et al., Dominant negative suppression of Rad leads to QT prolongation and causes ventricular arrhythmias via modulation of L-type $Ca^{2+}$ channels in the heart, Circ. Res. 101 (2007) 69–77.
[10] L. Chang, J. Zhang, Y.-H. Tseng, C.-Q. Xie, J. Ilany, J.C. Brüning, et al., Rad GTPase deficiency leads to cardiac hypertrophy, Circulation 116 (2007) 2976–2983.
[11] G. Wang, X. Zhu, W. Xie, P. Han, K. Li, Z. Sun, et al., Rad as a novel regulator of excitation–contraction coupling and β-adrenergic signaling in heart, Circ. Res. 106 (2010) 317–327.
[12] E. Picht, J. DeSantiago, S. Huke, M.A. Kaetzel, J.R. Dedman, D.M. Bers, CaMKII inhibition targeted to the sarcoplasmic reticulum inhibits frequency-dependent acceleration of relaxation and $Ca^{2+}$ current facilitation, J. Mol. Cell. Cardiol. 42 (2007) 196–205.
[13] K.B. Andersson, J.A.K. Birkeland, A.V. Finsen, W.E. Louch, I. Sjaastad, Y. Wang, et al., Moderate heart dysfunction in mice with inducible cardiomyocyte-specific excision of the SERCA2 gene, J. Mol. Cell. Cardiol. 47 (2009) 180–187.
[14] L.-S. Song, S.-Q. Wang, R.-P. Xiao, H. Spurgeon, E.G. Lakatta, H. Cheng, β-Adrenergic stimulation synchronizes intracellular $Ca^{2+}$ release during excitation–contraction coupling in cardiac myocytes, Circ. Res. 88 (2001) 794–801.
[15] L.-S. Song, E.A. Sobie, S. McCulle, W.J. Lederer, C.W. Balke, H. Cheng, Orphaned ryanodine receptors in the failing heart, Proc. Natl. Acad. Sci. U.S.A. 103 (2006) 4305–4310.
[16] S.O. Marx, S. Reiken, Y. Hisamatsu, T. Jayaraman, D. Burkhoff, N. Rosemblit, et al., PKA phosphorylation dissociates FKBP12.6 from the calcium release channel (ryanodine receptor): defective regulation in failing hearts, Cell 101 (2000) 365–376.
[17] M. Scoote, A.J. Williams, The cardiac ryanodine receptor (calcium release channel): emerging role in heart failure and arrhythmia pathogenesis, Cardiovasc. Res. 56 (2002) 359–372.
[18] X. Xu, S.O. Marx, H.M. Colecraft, Molecular mechanisms, and selective pharmacological rescue, of Rem-inhibited $Ca_V1.2$ channels in heart, Circ. Res. 107 (2010) 620–630.